Journal of Education and Science (ISSN 1812-125X)

Preparation of Zinc Oxide via Chemical Spray Pyrolysis and Investigation of Its Optical Properties

D. D. Ablahad [1], M. S. H. Al-Jubbori [2*]

[1,2] Department of Physics, College of Education for Pure Sciences, University of Mosul, Mosul, Iraq

Article information

Article history:
Received: February 15, 2026
Revised: May 02, 2026
Accepted: May 09, 2026
Available online: July 01, 2026

Keywords:
Zinc Oxide
Chemical Spray Pyrolysis
Absorption Coefficient
Energy Gap

Correspondence:
Mutaz Salih Hasan Al-Jubbori
mutazaljuboori@uomosul.edu.iq

Abstract

In this paper, structural and optical properties of zinc oxide thin films prepared by the chemical spray pyrolysis technique were studied. The deposition process involved spraying a transparent chemical solution made from zinc nitrate dissolved in distilled water at a temperature of 50° C on a square glass substrate measuring 2.5 cm. The deposition process was conducted at 350° C and a pressure of 2 bar. The optical properties of zinc oxide were studied using UV-Vis across a wavelength range from 190 nm to 1100 nm. The result showed that the absorption values are more recognised in the ultraviolet region, between (375-380) nm, followed by a sharp decrease in the visible and infrared light regions, where the material exhibited high transparency. Moreover, the result showed that the same change occurred with the absorption coefficient, refraction, extinction, and other optical constants as a function of the wavelength for zinc oxide films. The energy gap of the zinc oxide films was found to be (3.25 eV) at the same temperature. X-ray diffraction (XRD) measurement showed that the structure of the zinc oxide material is pure and hexagonal. This analysis helped us to calculate the average crystallite size, which was found to be approximately 44.34 nm, the lattice constants a = b 3.2190 Å and c=5.1490 Å, the cell volume 46.21 $\times 10^{6}$ pm^3, the X-Ray density 5.85 g/cm3 of ZnO sample, the thickness of the film 300 nm, and the number of layers $N_L = 6.7658$, the density of dislocations $\delta = 5.086 \times 10^{-4}$ nm^{-2}, the number of crystals $N_{\circ} = 3.44 \times 10^{11} cm^{-2}$ and the Specific Surface Area $SSA = 24.138$ m^2 /g.

DOI: 10.33899/jes.v35i3.61594, ©Authors, 2026, College of Education for Pure Science, University of Mosul.

1. Introduction

Since the beginning of the 20th century, the industry has tended towards the development of products that are low-cost, efficient, and small-sized. Because the use of bulk semiconductors in the manufacture and production of electronic devices is expensive, attempts have been made to replace these devices with layers of membranes. Therefore, researchers have developed methods for depositing membranes and discovered new methods as well, as the physical properties of the manufactured membranes vary according to the nature of the deposition method used [1]. This technique has significantly contributed to the development of semiconductor research, as it provides methods for studying the physical and chemical properties of materials in a better and easier way than if the material were in its bulk state. It is an important branch of solid state physics and is concerned with micro and nano devices that have very thin dimensions [2]. The choice of deposition method depends on several factors, including production cost and the field in which it is used, by controlling the specifications of the formed membrane, which depends on the quality of the materials used and the type of base on which it is deposited. There are several deposition methods, from which we chose the chemical vapour deposition method because it is inexpensive and easy to deposit membranes, depending on the components of the simple system, and because the membranes formed in this way are characterised by homogeneity and stability of their physical properties over time [3].

Zinc oxide was chosen because it is considered a semiconductor with a large energy gap (3.37 eV) at room temperature, and a large exciton binding energy of 60 meV [4]. This energy ensures high emission efficiency at room temperature by reducing the threshold energy for ultraviolet lasers. Moreover, it shows excellent thermal performance and high chemical stability. In the visible light region, it exhibits high transmittance [5], which makes it suitable for use in thermal mirrors. Furthermore, its electrical properties make it suitable for light-emitting display devices [6-7]. Due to these properties, it is used in solar cells, sensors, and photodetectors [8-9]. On the other hand, owing to its distinctive optical and electronic properties, this material has gained particular importance in the manufacture of various electro-optical devices. Moreover, zinc oxide is used in data storage and in solar cells as an anti-reflective coating. Due to its minimal impact on the environment, it is used in electromagnetic devices [10]. Furthermore, it is used as a photothermal conversion system and as semiconductor multilayer coatings in gas sensors and optical position sensors [11-12-13]. Zinc oxide exhibits high chemical stability, chemical sensitivity to various absorbable gases, susceptibility to contamination, and non-toxicity [14]. It is considered a promising material in the manufacture of ultraviolet and blue light-emitting devices and surface acoustic wave devices [15]. Therefore, this work aims to study the optical properties of nanostructured zinc oxide thin films to understand their electronic and optical behaviour, analyse the effect of preparation conditions on film quality and performance, and evaluate the suitability of this material for practical applications.

2. EXPERIMENTAL DETAILS

2.1. Preparation of glass substrate

We used glass made in China, Al Malak Company; the slides were cut with an area of 2.5 × 2.5 cm and 1 mm thick. In order to obtain a surface free of impurities, we cleaned the base thoroughly to obtain accurate results. The glass bases were washed thoroughly with distilled water and then placed in an ultrasonic cleaning device with acetone and distilled water for 20 minutes at a temperature of 30° C. The glass pieces were then dried using a lens cleaning cloth, placed in boxes to protect them from contamination, and left for 24 hours to dry completely before using.

2.2. Preparation of the solution

The solution was prepared using zinc nitrate, a white crystalline substance with the chemical formula [$Zn(NO_3)_2$] [M. W =297.48 gm/m], at a concentration of (0.3 M), which is recommended in reference [16], by adding a quantity of the substance weighed with a sensitive electronic balance at (8.9244 gm) to (100 mL) of distilled water. Then, it was placed on a magnetic mixer for 60 minutes at a temperature of 50°C in order to obtain a homogeneous solution free of lumps and ensure that it dissolved well, with a transparent colour after dissolving in distilled water. Filtration paper was then used to remove impurities and obtain a high-purity solution.

2.3. Deposition process

After cleaning and sterilising the bottles, they were placed on an electric heater, and the temperature regulator was set to 350° C. The air pressure in the sprayer was set to 2 bar. The prepared solution is placed in the nozzle at a height of 30 cm from the base on which the glass plates are placed. The spraying process takes place during 40 sprays consecutively, and the duration of single spray is 10 sec ± 1, and the time between one splash and the next 180 sec and the flow rate of the solution is 4 mL/min, until the desired zinc oxide film is obtained, as shown in **Figure 1.**

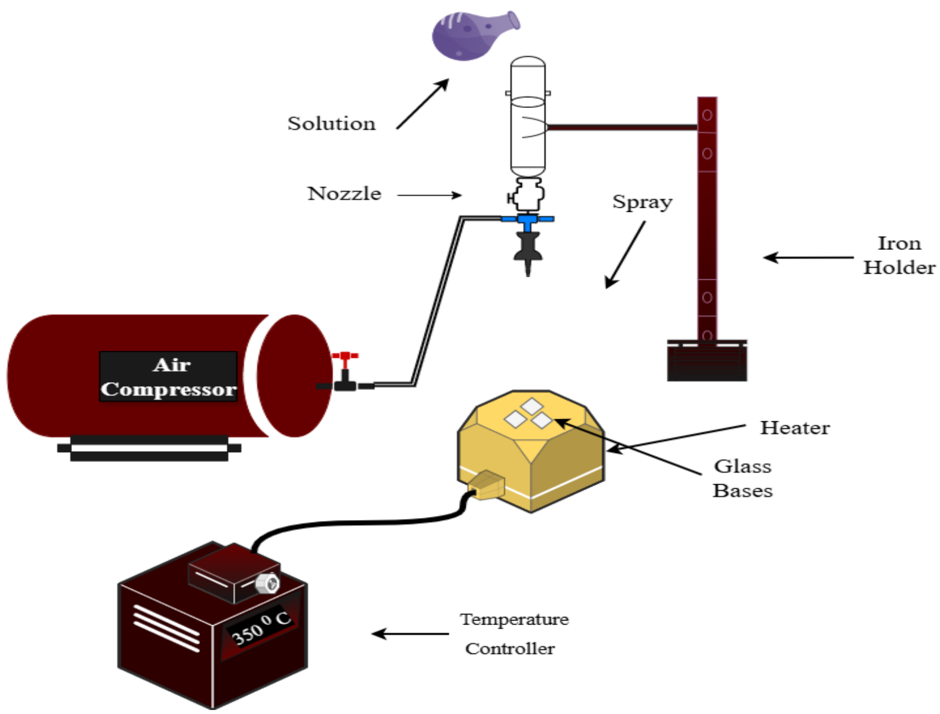

Figure 1: Spraying system

3. RESULTS AND DISCUSSIONS

3.1. X-ray Diffraction (XRD)

This technique is used to determine the structure of crystalline materials, as X-rays scatter at specific angles and appear as peaks on a graph when they fall on a crystalline sample. The unique diffraction pattern of a material allows for the study of the sample purity and identity. A device of the (MALVERN PANALYTICAL-AERIS) type, jointly operated by two countries (the Netherlands and the United Kingdom), located in Baghdad's Yarmouk district at the Al-Khorah centre for Nanotechnology, was used. We concluded that this material is zinc oxide with a hexagonal structure based on Miller indices, which represent the different directions of crystallisation within the crystal. The greatest consistency in orientation was found in the (002) direction when compared with the other orientations, indicating that this is the predominant orientation of the prepared films, which is consistent with the hexagonal structure of zinc oxide material. The other main peaks confirm the crystalline structure. The result showed that the sample exhibited large crystals, as indicated by the narrow and sharp peaks, and that the material is also of high purity due to the presence of peaks specific to zinc oxide. The average crystallite size of the zinc oxide thin films was calculated from the Debye-Scherrer **eq.(1)[17]**:

$$\mathbf{D_{AV}} = \frac{k\lambda}{\beta cos\theta_B} \dots\dots\dots\dots\dots\dots\dots\dots\dots\dots (1)$$

Where $\mathbf{D_{AV}}$ is the average crystallite size, λ is the X-ray wavelength, k is the shape factor, which is a constant taken as 0.9, β is the full width of the diffraction line at half its maximum intensity, and θ_B represents the Bragg angle.

For a hexagonal (wurtzite structure), the lattice constants a and c can be calculated using Bragg's law. The lattice constants are related to the Miller indices by the following **eq. (2)[17]**:

$$\frac{1}{d^2} = \frac{3}{4} \times \frac{h^2 + hk + k^2}{a_\circ^2} + \frac{l^2}{c_\circ^2} \dots\dots\dots\dots\dots\dots\dots\dots\dots\dots (2)$$

Where (a,b,c) are lattice parameters, (h, k, l) are the Miller indices, and d Interplanar spacing.
And d can be calculated from Bragg's **eq.(3) [17]**:

$$n\lambda = 2d \sin\theta \dots\dots\dots\dots\dots\dots\dots\dots\dots\dots (3)$$

where n is the order of reflection.
The cell volume of a hexagonal unit cell can be calculated using the lattice constants a and c by the following **eq. (4) [17]**:

$$V = \frac{\sqrt{3}}{2} a_\circ^2 . c_\circ \dots\dots\dots\dots\dots\dots\dots\dots\dots\dots (4)$$

Where V is the cell volume.

The X-ray density of the ZnO sample was calculated by using the **eq. (5)** [18]:

$$D_x = \frac{nM}{N_A V} \dots\dots\dots\dots\dots\dots\dots\dots\dots\dots (5)$$

where D_x is X-ray density, n is the number of atoms per unit cell, M is the molecular weight of the sample (M= 81.38 g/mol) for the ZnO, and N_A is Avagadro's number.

The thickness of the film was calculated using the following **eq. (6)** [19]:

$$t = \frac{\Delta W}{\rho \times A} \dots\dots\dots\dots\dots\dots\dots\dots\dots\dots (6)$$

where (ΔW) represents the difference in weight of the glass substrate before and after deposition, (t) is the thickness of the deposited film, (A) is the area of the film, and (ρ) is the density of the film material.

The number of layers N_L, the density of dislocations δ, the number of crystals $N_\circ$ and the specific surface area (SSA) was calculated using the following **eq. (7**) [20], **eq. (8**)[21]**, eq. (9)** [22] and eq. (10) [23] respectively:

$$N_L = \frac{t}{D} \dots\dots\dots\dots\dots\dots\dots\dots\dots\dots (7)$$

$$\delta = \frac{1}{D^2} \dots\dots\dots\dots\dots\dots\dots\dots\dots\dots (8)$$

$$N_\circ = \frac{t}{D^3} \dots\dots\dots\dots\dots\dots\dots\dots\dots\dots (9)$$

$$SSA = \frac{S_V}{\rho} \dots\dots\dots\dots\dots\dots\dots\dots\dots\dots (10)$$

Where S_V represents the surface density and can be calculated using the **eq. (11) [24]** and (K_{SV}) is a constant representing the shape factor.

$$S_V = \frac{K_{SV}}{D_{av}} \dots\dots\dots\dots\dots\dots\dots\dots\dots\dots (11)$$

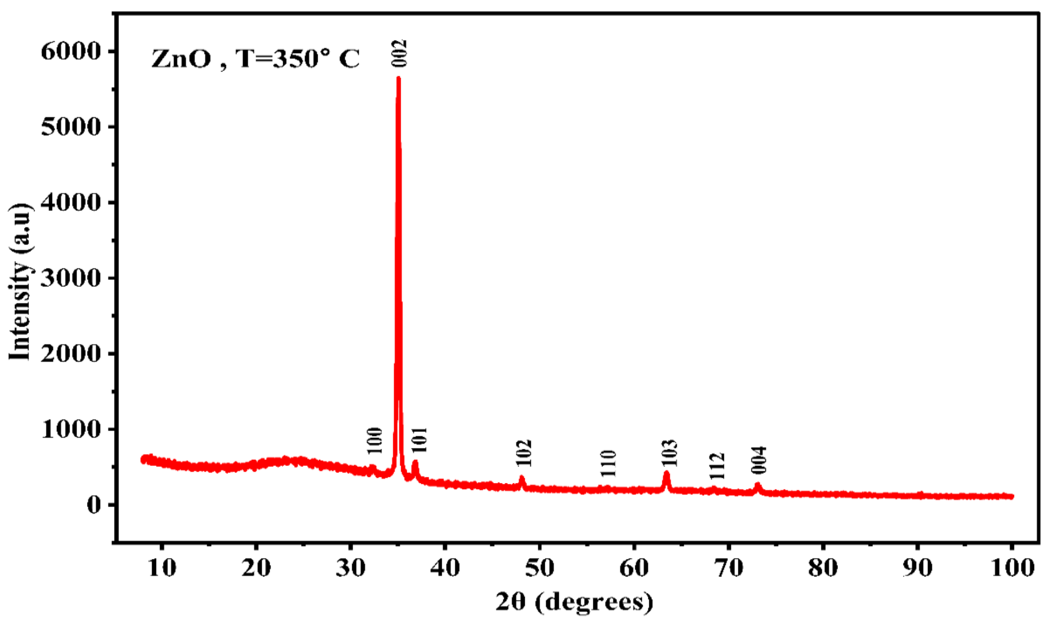

Figure 2 X-ray diffraction of ZnO thin films for substrate temperature 350 ºC.

3.2. The Optical absorption analysis

To learn more about the optical properties of thin zinc oxide films, the interaction of light with them was analysed using an ultraviolet-visible (UV-Vis) spectrophotometer (Shimadzu UV-1800), where the wavelength range of the absorption spectrum ranged between 190 and 1100 nm at a scanning rate of 400 nm/min. minute. The result showed that light is absorbed by the thin films deposited on the glass substrates, compared to the wavelength spectra of zinc oxide films at a temperature of 350 °C when light interacted with the thin film.

3.2.1 Absorption

Figure 3 shows the relationship between absorptivity and wavelength for a sample of zinc oxide thin film deposited at 350°C. The shape of the curve shows the absorption peak representing the band gap of zinc oxide and appearing at short wavelengths between (375-380) nm. Due to the transition of electrons from the valence band to the conduction band, the material absorbs light falling on it at this wavelength. After this peak and with increasing wavelength, the result showed a rapid decrease in absorptivity, indicating that the material is relatively transparent in the visible region. This makes materials with these characteristics suitable for use in optical sensors, solar cells, and photostimulation applications. The material is also suitable for optical and electronic devices due to its high absorption in the ultraviolet region [25].

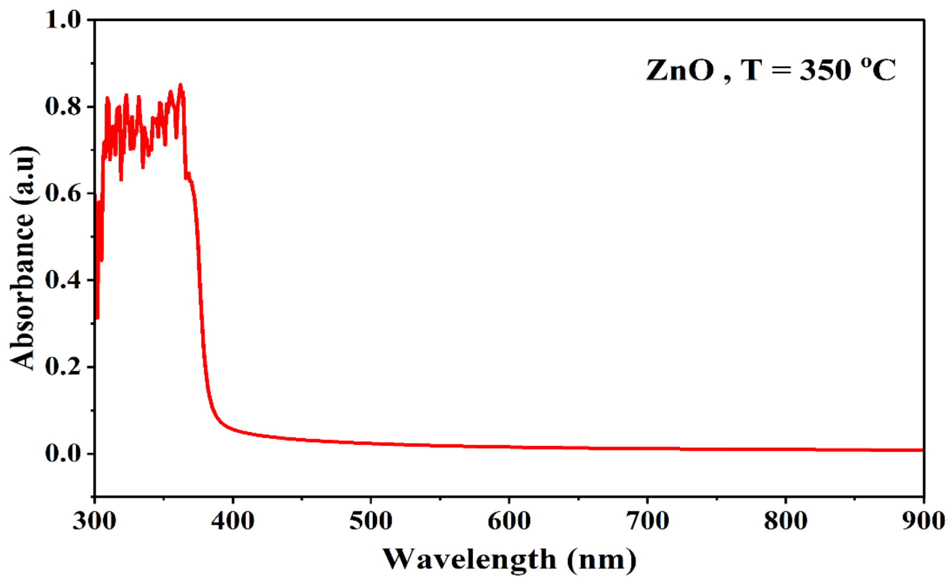

Figure 3 Change in the absorption spectrum as a function of wavelength for zinc oxide (ZnO) thin films.

3.2.2 Absorption coefficient

The absorption coefficient depends on the type of electronic transitions and energy gap, as well as on the properties of semiconductors and the energy of the incident photon. It can be seen from **Figure 4**, which shows the absorption coefficient as a function of wavelength, that the absorption coefficient decreases significantly with increasing wavelength until it stabilises in the visible spectrum, these results are consistent with [26],. We can calculate the absorption coefficient using the following **eq.(12)** [27] :

$$\alpha = 2.303\frac{A}{t} \dots\dots\dots\dots\dots\dots\dots\dots\dots\dots (12)$$

Where α is absorption coefficient and A is the absorbance.

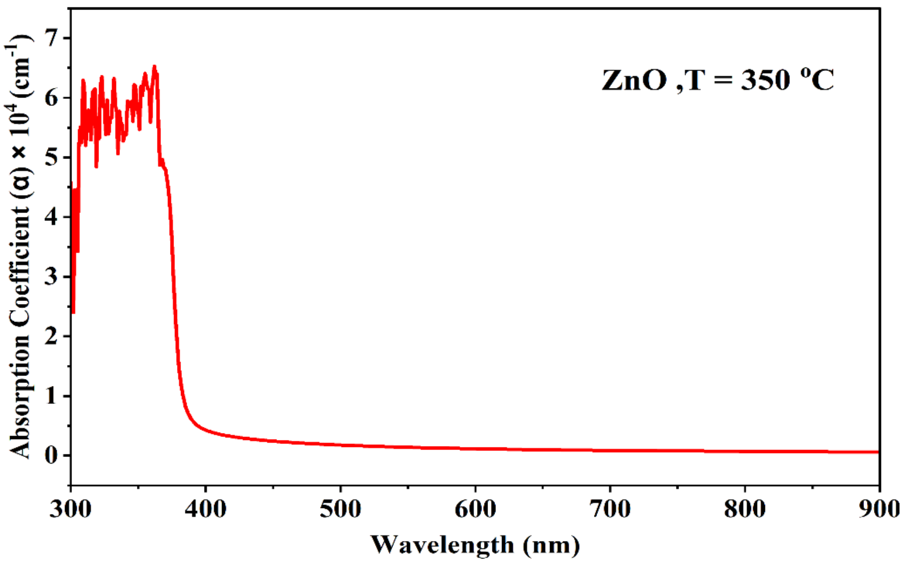

Figure 4: Absorption coefficient of ZnO thin films as a function of wavelength.

3.2.3 Energy gap

Figure 5 shows the optical band gap of zinc oxide at a temperature of 350 °C. This graph represents the band gap diagram used for semiconductors to determine their energy gap. The result showed that the energy gap is (3.25) eV, which is very close to the energy gap of zinc oxide at room temperature (3.37 eV). This slight decrease in the energy gap is attributed to the high deposition temperature of this material, where a change in the electronic structure occurs due to the effect of thermal expansion. However, the material retained its properties as a semiconductor with a wide and direct energy gap even at high temperatures, making it more suitable for advanced optical and electronic applications that require thermal stability. We use **eq. (13)** to calculate the energy gap according to the following expression [28]:

$$(\alpha . hv)^{n} = k\left(hv - E_{g}^{opt.}\right) \quad \ldots\ldots\ldots\ldots\ldots\ldots\ldots\ldots\ldots\ldots (13)$$

Where (k) is a constant that depends on the nature of the material, (hv) represents the photon energy, ($E_g^{opt.}$) denotes the optical band gap, and n is an exponent that is dependent on the nature of the allowed or forbidden electronic transitions. Thus, for allowed direct transition n = 1/2, whereas n = 3/2 describes the case for forbidden direct transition, n = 2 indicates indirect allowed transition and n = 3 indicates indirect forbidden transitions. Since ZnO is a direct band gap semiconductor with a hexagonal wurtzite crystal structure, as confirmed in the XRD measurements, n = 1/2 [29].

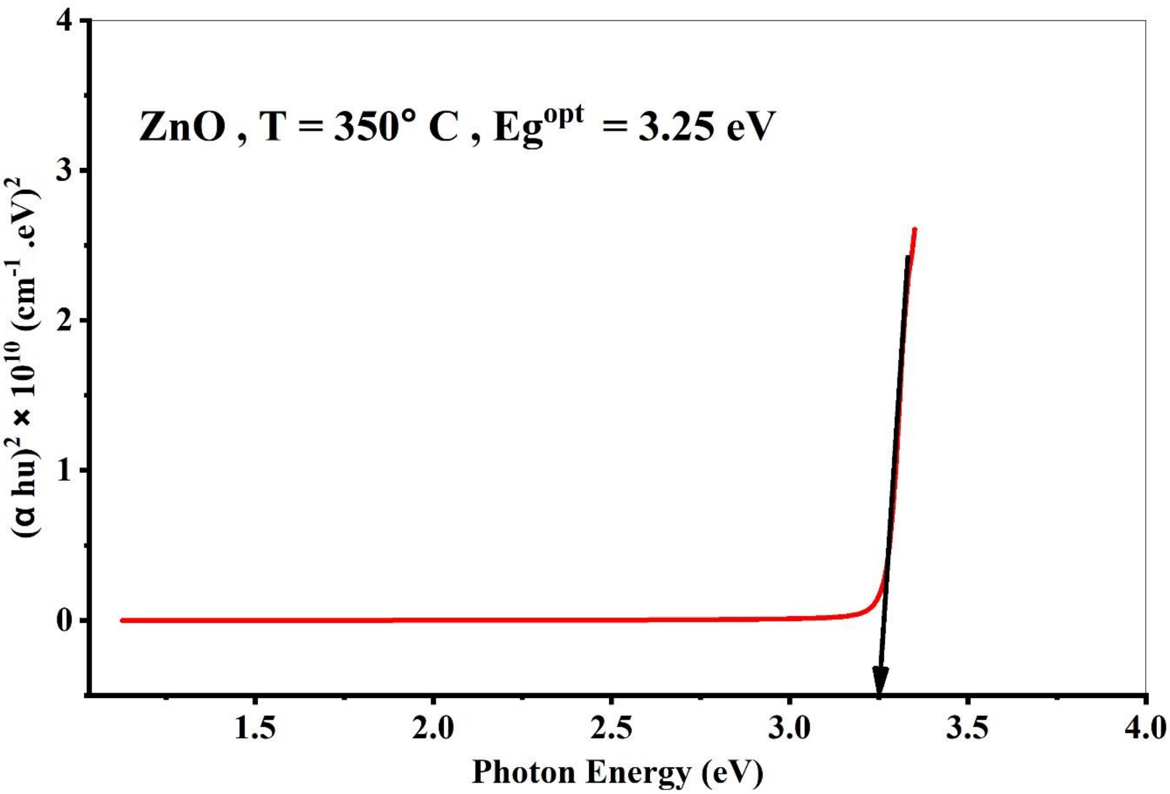

Figure 5 Optical band gap values for prepared ZnO thin films.

3.2.4 Refractive index

The refractive index can be defined as the ratio of the speed of light in a vacuum and its speed in a physical medium, which describes how light propagates through a transparent medium. It depends on the type of material and crystal structure, and can be calculated using the following **eq.(14)** [6]:

$$n = \sqrt{\frac{4R}{(R-1)^2} - K^2} - \left(\frac{R+1}{R-1}\right) \dots\dots\dots\dots\dots\dots\dots\dots\dots (14)$$

Where (n) is the refractive index, (K) is the extension coefficient and (R) is the reflectivity which can be found using the following **eq.(15)** [30]:

R = 1 - T – A ………………….(15)

Where (T) is the transmittance and (A) refers to the absorbance. **Figure 6** shows the spectral relationship between wavelength and refractive index, where it is at its highest value at short wavelengths and gradually decreases with increasing wavelength.

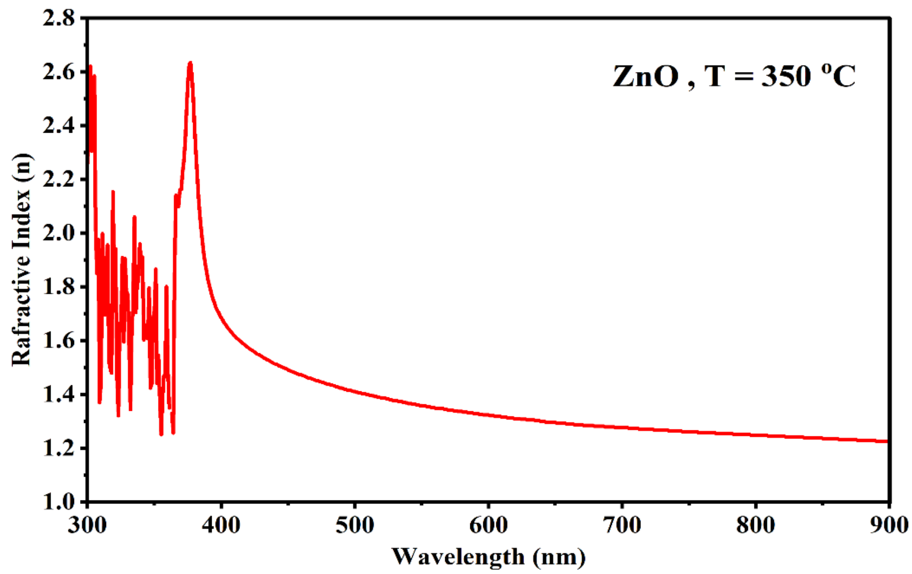

Figure 6: Refractive index function of wavelength for ZnO thin films.

3.2.5 Extinction coefficient

The extinction coefficient is one of the important optical constants which expresses the amount of attenuation in the electromagnetic wave as it travels through matter. When its value is high, it indicates strong absorption of photons, while when its value is low, it indicates high transparency of matter. From **Figure 7**, we can see that the extinction coefficient is high at short wavelengths, reflecting strong absorption of high-energy photons near the edge of the energy gap. The extinction coefficient decreases with increasing wavelength, and the absorption decreases, and this region becomes optically transparent. We can calculate the extinction coefficient using the following **eq.(16)** [3]:

$$K = \frac{\alpha\,\lambda}{4\pi} \ldots\ldots\ldots\ldots\ldots\ldots\ldots\ldots\ldots\ldots (16)$$

Where (λ) is the wavelength and (π) is a mathematical constant.

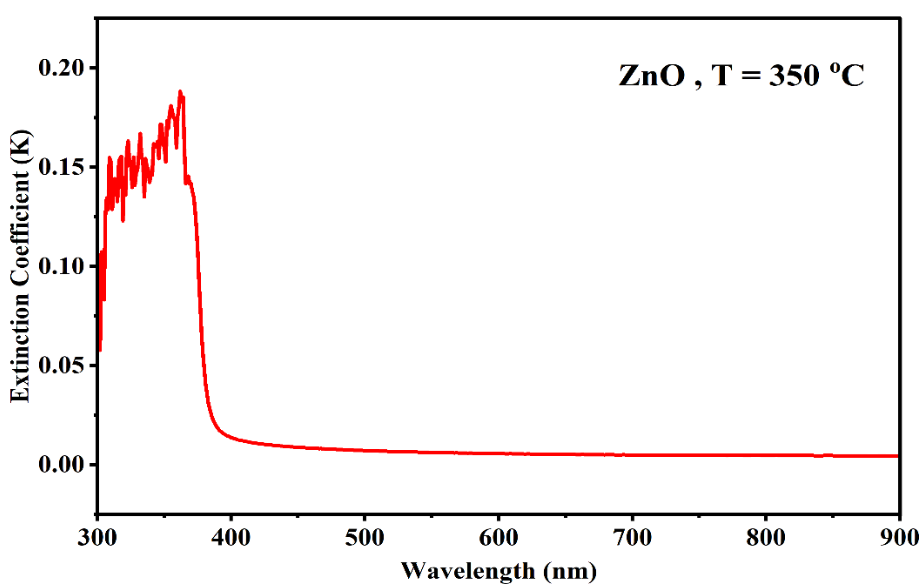

Figure 7: Extinction coefficient as a function of wavelength for ZnO thin films.

3.2.6 Real dielectric constant

Real dielectric constant is a measure of a material's ability to store energy from an applied electric field instead of losing and dissipating it. It can be seen from **Figure 8** that the real dielectric constant decreases with increasing wavelength, a behaviour known as natural dispersion. High values at short wavelengths indicate the material's ability to polarise charges when exposed to high-energy light. This result is consistent with [31]. It can be defined using Maxwell's equations in electromagnetism, which relates it to the refractive index according to the following **eq. (17)** [32]:

$\varepsilon_r = n^2 - K^2$ … … … … … … … … … … … (17)

Where (ε_r) is the real dielectric constants.

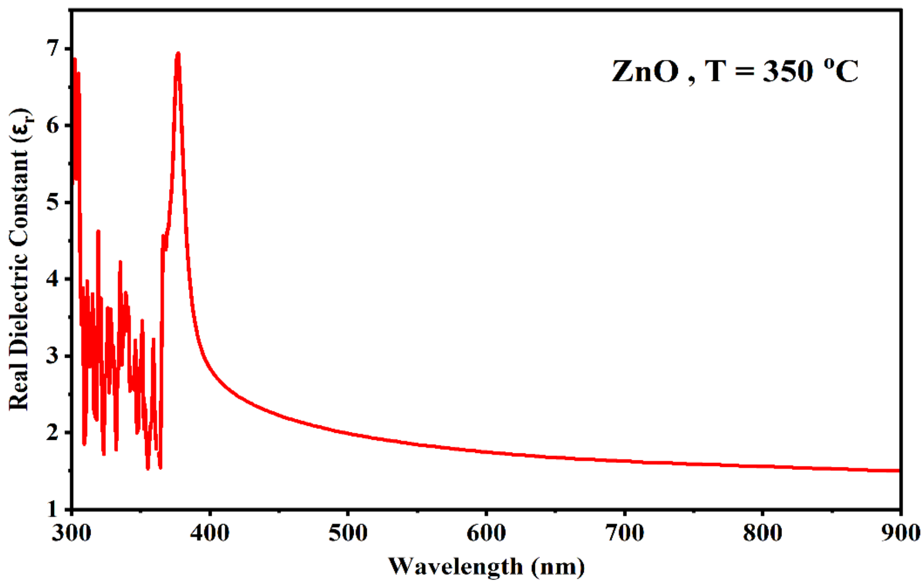

Figure 8: Real dielectric constants as a function of wavelength for ZnO.

3.2.7 Imaginary dielectric constant

The imaginary dielectric constant represents the amount of energy absorbed by the material from the light falling on it. **Figure 9** shows that the imaginary dielectric constant of the prepared zinc oxide decreases with increasing wavelength, indicating that the material has low absorptivity in the near-infrared region and high absorptivity in the visible spectrum. This is typical behaviour for semiconductors as reported in [33]. It can be calculated from Maxwell's equation for electromagnetism according to the following **eq.(18)** [32]:

$\varepsilon_i = 2nK$ … … … … … … … … … … … (18)

Where (ε_i) is the imaginary dielectric constant**.**

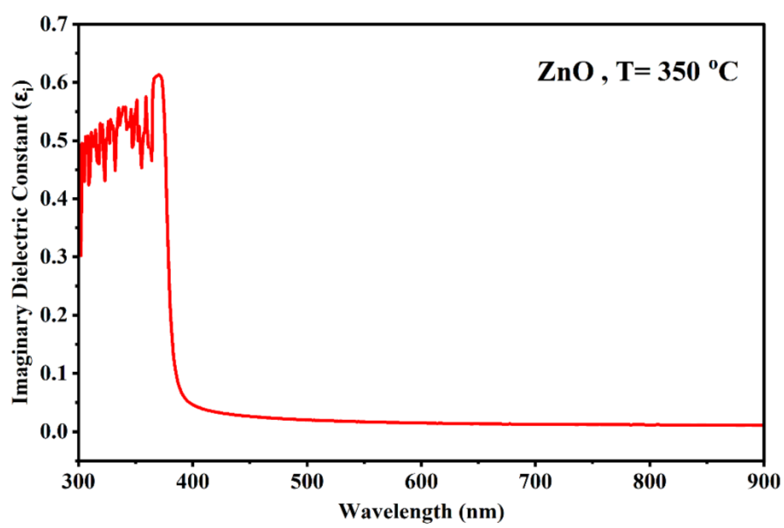

Figure 9: Imaginary dielectric constants as a function of wavelength for ZnO.

3.2.8 Optical conductivity

Figure 10 shows the optical conductivity of the prepared zinc oxide as a function of the wavelength. The result showed a gradual decrease with increasing wavelength, which is consistent with [34]. The optical conductivity can be calculated using the following **eq.(19)** [32]:

$$\sigma_{opt.} = \frac{\alpha\, n\, c}{4\pi} \dots\dots\dots\dots\dots\dots\dots\dots\dots\dots (19)$$

Where ($\sigma_{opt.}$) is the optical conductivity and (c) is the speed of light.

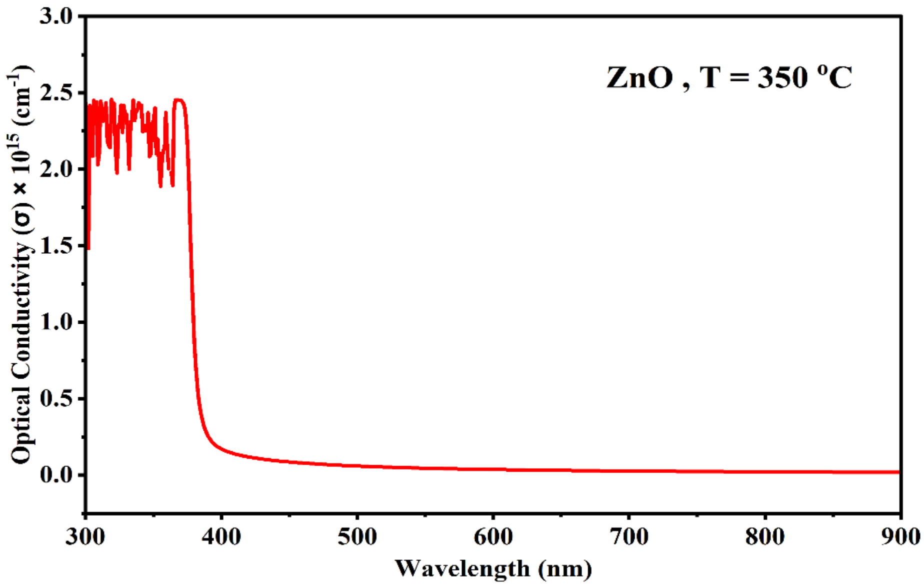

Figure 10: Optical conductivity as a function of wavelength for ZnO.

For a more detailed comparison with other studies, see Tables 1 and 2, where it is noted that the average crystal size of the sample is found to be 44.34 nm at 350° C. Moreover, the lattice constants a and c, the cell volume, the X-Ray density of the ZnO sample, the thickness of the film, and the number of layers N_L, the density of dislocations δ, the number of crystals $N_\circ$ and the specific surface area (SSA) was also calculated, and their values are shown in Table 1.

Table .1. The parameters calculated from the XRD data are presented

detailed analysis	Present work		References
a = b	3.2190 Å	3.245 Å	[Shimpi et al.,2021][21]
c	5.1490 Å	5.209 Å	
the density of dislocations (δ)	5.086 × 10-4 nm^{-2}	5.859 × 10-4 nm^{-2}	
The average crystallite size(D_{av})	44.34 nm	41.31 nm	
Volume of cell V	46.21 $\times 10^6$ pm^3	47.77 $\times 10^6$ pm^3	[Mobarak et al., 2025][23]
the Specific Surface Area (SSA)	24.138 m^2 /g	32.58 m^2 /g	
The X-Ray density (D_x)	5.85 g/cm3	5.607 g/cm3	[Khlifi et al.,2024][18]
the band gap	(375-380) nm	(360- 380) nm	[Darji et al., 2025][35]

Table .2. comparison table of the researchers work and previous studies

Rererence	Present work	[Qamo and Mimouni,2020][36]	[Rahmani and Wasaa,2017][37]	[Chadala, 2016][38]
The temperature of preparation	350 °C	350 °C	485 °C	375 °C
The thickness of the film (t)	300 nm	223 nm	252.9 nm	507.764 nm
Energy gap (E_g)	3.26 eV	3.24 eV	3.25 eV	3.214 eV
Refractive index (n) in (550 nm)	1.41	1.67	1.8812	1.656
extinction coefficient K	1×10^{-2}	9.79×10^{-4}	_---_	---

4. Conclusion

Thin hexagonal zinc oxide films were successfully prepared using a simple, cost-effective and rapid chemical spray method. The optical properties showed that the conductivity, absorption coefficient, refractive index, extinction coefficient, and real and imaginary insulation constants were all decreased with increasing wavelength. The energy gap of the sample was found to be 3.25 eV at 350° C. It was calculated by drawing a tangent to the curve and projecting it onto the photon energy axis, where its value corresponded to the range of zinc oxide. The average crystal size of the sample was found to be 44.34 nm at 350° C. Moreover, the lattice constants a and c, the cell volume, the X-Ray density of the ZnO sample, the thickness of the film, and the number of layers N_L, the density of dislocations δ, the number of crystals $N_{\circ}$ and the specific surface area (SSA) was also calculated, and their values are shown in Table 1.

5. Acknowledgments

The authors would like to express their appreciation to warmest thanks to the University of Mosul, College of Education for Pure Science, Department of Physics for supporting this work. for supplying the materials for this study. Special thanks go to Ivan B. Karomi, Cardiff University, UK, for his proofreading of this paper.

6. Declarations

The authors declare that they have no known competing financial interests or personal relationships that could have appeared to influence the work reported in this paper.

6.1 Ethics approval and consent to participate

Not applicable.

6.2 Consent for publication

I agree

6.3 Availability of Data and Materials

Data will be provided upon receiving a valid request.

6.4Conflicts of interest

The authors declare that there is no conflict of interest

6.5 Funding

The authors declare that they have no known competing financial interests or personal relationships that could have appeared to influence the work reported in this paper.

7 . References

[1] Aswad TA, Jamil NY, Ibrahim AM, "Effect of deposition time and temperature on structural, topographic and optical properties of nano ZnS film prepared by CBD technique," Raf. J. Sci., vol. 28, no. 4, pp. 94–105, 2019, doi: 10.33899/rjs.2019.163304.

[2] Abdullah MN, "The effect of doped and undoped ZnO-V thin films on nanostructural and optical properties," Raf. J. Sci., vol. 34, no. 2, pp. 62–71, 2025, doi: 10.33899/rjs.2025.187745.

[3] Ayed O, Al-Jubbori MA, Algdirree HH, "Study of the optical properties of copper oxide thin films prepared by chemical spray pyrolysis technique," J. Edu. Sci., vol. 33, no. 2, pp. 47–57, 2024, doi: 10.33899/edusj.2024.146903.1426.

[4]Aoun Y, Benhaoua B, Gasmi B, Benramache S, “Structural, optical and electrical properties of zinc oxide (ZnO) thin films deposited by a spray pyrolysis technique,” J. Semicond., vol. 36, no. 1, 2015, doi: 10.1088/1674-4926/36/1/01xxx.
[5]Ahmad IA, Mohammed YH, Abbas KN, “Effect of evaporation boat-substrate distance on the formation of zinc oxide nanostructures,” J. Edu. Sci., vol. 31, no. 3, pp. 147–164, 2022, doi: 10.33899/edusj.2022.134805.1262.
[6]Sinjar MS, Al-Jubbori MA, Algdirree HH, “Study of the effect of irradiation on some optical properties of cadmium oxide films prepared by the thermal chemical spraying method,” J. Edu. Sci., vol. 34, no. 2, pp. 1–12, 2025, doi: 10.33899/edusj.2024.154469.1511.
[7]Al-dory AAH, Al-juboori MSH, “Study the effect of annealing on some physical properties of ZnO and NiO nanostructures,” J. Edu. Sci., vol. 30, no. 4, pp. 37–58, 2021, doi: 10.33899/edusj.2021.129592.1144 .
[8]Inamdar SI, Ganbavle VV, Rajpure KY, “ZnO based visible–blind UV photodetector by spray pyrolysis,” Superlattices Microstruct., vol. 76, pp. 253–263, 2014, doi: 10.1016/j.spmi.2014.09.041.
[9]Kareem AA, Aljawadi YA, Zaker TA, “Nonlinear optical properties of pure ZnO and Sn, Al doped and co-doped ZnO thin films using Z-scan technique,” Raf. J. Sci., vol. 34, no. 3, pp. 79–90, 2025, doi: 10.33899/rjs.2025.189220.
[10]Mohammed HN, “Performance analysis of n-ZnO/p-Si heterojunction diode as function of zinc oxide thin films thickness,” J. Edu. Sci., vol. 31, no. 2, pp. 114–127, 2022, doi: 10.33899/edusj.2022.133482.1227.
[11] Zafariney ZA, Johari S, Ismail MH, Aris H, Zakaria MR, “Comparative study on the structural and morphological properties of ZnO thin films prepared by different deposition techniques,” Proc. SPIE, vol. 14059, 1405907, 2026, doi: 10.1117/12.3070175.
[12] Rincon-Suarez E, Mozo JM, Romero-López A, Alcántara-Iniesta S, Flores-Ruiz FJ, Serrano LE, “Structural, optical and electrical properties of ZnO thin films deposited in the plane direction (002) by ultrasonic spray pyrolysis using nitrogen as carrier gas,” Mater. Sci. Eng. B, vol. 320, 118430, 2025, doi: 10.1016/j.mseb.2025.118430.
[13] Al-Jubbori MA, Sinjara MS, Saleh A, “Chemical spray pyrolysis of cadmium oxide thin films: UVC-induced structural and optical modifications for enhanced photodetector performance,” Opt. Mater., vol. 168, 117430, 2025, doi: 10.1016/j.optmat.2025.117430.
[14] Nisha R, Madhusoodanan KN, Vimalkumar TV, Vijayakumar KP, “Gas sensing application of nanocrystalline zinc oxide thin films prepared by spray pyrolysis,” Bull. Mater. Sci., vol. 38, no. 3, pp. 1–9, 2015, doi: 10.1007/s12034-015-1046-1.
[15] Mousa AO, Habubi NF, Nema NA, “Substrate effects on structural and optical properties of ZnO thin films deposited by chemical spray pyrolysis,” Int. Lett. Chem. Phys. Astron., vol. 51, pp. 69–77, 2015, doi: 10.18052/www.scipress.com/ILCPA.51.69**.**
[16] Zaier A, Oum El az F, Lakfif F, Kabir A, Boudjadar S, Aida MS, “Effects of the substrate temperature and solution molarity on the structural opto-electric properties of ZnO thin films deposited by spray pyrolysis,” Mater. Sci. Semicond. Process., vol. 12, no. 6, pp. 207–211, 2009, doi: 10.1016/j.mssp.2009.12.002.
[17] Huong TTT, Sa NT, Thuy NTM, Hao PV, Thao NH, Hien NT, Ca NX, “Eu^{3+}-doped ZnO quantum dots: structure, vibration characteristics, optical properties, and energy transfer process,” Nanoscale Adv., vol. 7, pp. 909–921, 2025, doi: 10.1039/D4NA00858H.
[18] Khlifi N, Ihzaz N, Toulemonde O, Dandre A, Labrugère-Sarroste C, Bessadok MN, Lemine OM, El Mir L, “Cobalt-doped ZnO nanoparticles and PLD-deposited thin film forms: structure, optical properties and nature of magnetic anisotropy,” RSC Adv., vol. 14, no. 38, pp. 27622–27633, 2024, doi: 10.1039/D4RA05021E.
[19] Al-Jubbori MA, Sinjar MS, Salih HA, Khalil AZ, Mohammed FA, Saleh A, “UVC-tuned cadmium oxide thin films via spray pyrolysis: structural evolution and photodetector efficiency,” Appl. Phys. A, vol. 132, 188, 2026, doi: 10.1007/s00339-026-09378-5.
[20] Al-Jabiry AJ, “Studying the effect of molarity on the physical and sensing properties of zinc oxide thin films prepared by spray pyrolysis technique,” Ph.D. Thesis, Applied Sciences Department, University of Technology, Baghdad, Iraq, 2007.
[21] Shimpi NT, Ahirrao PB, “Fabrication of low cost photocell based nanostructured ZnO thin films on ITO substrates by chemical bath deposition method,” Int. J. Creat. Res. Think., vol. 9, no. 3, 2021, ISSN 2320-2882.
[22] Dhanam M, Prabhu RR, Manoj PK, “Investigations on chemical bath deposited cadmium selenide thin films,” Mater. Chem. Phys., vol. 107, pp. 289–296, 2008, doi: 10.1016/j.matchemphys.2007.08.095.
[23] Mobarak MB, Hossain MS, Chowdhury F, Tarannum N, Mesbah MB, Tanvir NI, Akhtar US, Ahmed S, “From discarded to desired: valorization of Zn–C battery waste into crystalline ZnO nanoparticles with crystallographic insights and antibacterial efficacy,” RSC Adv., vol. 15, pp. 38454–38469, 2025, doi: 10.1039/D5RA06684K.
[24] Pabst W, Gregorová E, “Characterization of particles and particle systems,” ICT Prague, Prague, Czech Republic, 2007.
[25] Ammaih Y, Lfakir A, Siadat M, “Structural, optical and electrical properties of ZnO:Al thin films for optoelectronic applications,” Opt. Quantum Electron., vol. 46, pp. 229–234, 2014, doi: 10.1007/s11082-013-9757-2.
[26] Virt I, Potera P, Gamernyk R, Cieniek B, “Structural and optical properties of Ni-doped ZnO thin films as TCO material, fabricated by pulsed laser deposition method,” Opt. Mater., vol. 154, 115643, 2024, doi: 10.1016/j.optmat.2024.115643.

[27] Khairallah NS, Al-Jubbori MA, Elzwam AE, "Study optical properties of nickel oxide syntheses by chemical spray pyrolysis," J. Edu. Sci., vol. 35, no. 2, pp. 57–67, 2026, doi: 10.33899/jes.v35i2.53669.
[28] Otieno F, Airo M, Erasmus RM, Billing DG, Quandt A, Wamwangi D, "Effect of thermal treatment on ZnO:Tb^{3+} nano-crystalline thin films and application for spectral conversion in inverted organic solar cells," RSC Adv., vol. 8, pp. 29274–29282, 2018, doi: 10.1039/C8RA04398A.
[29] Amrute V, Koroth SK, Manjhi MK, Monika, Upadhyaya CP, Vasundhara M, Chanda A, "Investigation of ZnO nanocomposites with 2-D derivatives of graphene for photocatalytic and antibacterial activities," J. Mater. Sci.: Mater. Eng., vol. 21, article no. 40, 2026, doi: 10.1186/s40712-026-00413-0.
[30] Qusay AA, Sanaa MA, "Study the optical properties of undoped and antimony doped tin oxide films prepared by APCVD technique," J. Edu. Sci., vol. 28, no. 3, pp. 228–236, 2019, doi: 10.33899/edusj.2019.162957.
[31] Calzolari A, Buongiorno Nardelli M, "Dielectric properties and Raman spectra of ZnO from a first principles finite-differences/finite-fields approach," Sci. Rep., vol. 3, 2999, 2013, doi: 10.1038/srep02999.
[32] Zhou Q, Ji Z, Hu B, Chen C, Zhao L, Wang C, "Structural properties of zinc oxide thin films," Mater. Lett., vol. 61, no. 2, pp. 531–534, 2007, doi: 10.1016/j.matlet.2006.05.004.
[33] Ibadat S, Younas M, Shahzada S, Nadeem M, Ali T, Akhtar MJ, Pollastri S, Rehman U-Ur, Yousef I, Khan RTA, "Realistic dielectric response of high temperature sintered ZnO ceramic: a microscopic and spectroscopic approach," RSC Adv., vol. 10, pp. 30451–30462, 2020, doi: 10.1039/D0RA04273K.
[34] Zhang XD, Guo ML, Li WX, Liu CL, "First-principles study of electronic and optical properties in wurtzite $Zn_{1-x}Cd_xO$," Comput. Mater. Sci. / related DFT optical properties study, vol. —, pp. —, 2013, doi: 10.7498/aps.62.047101.
[35] Darji J, Patel K, Jodhani K, "Green synthesis of zinc oxide nanoparticles using Peristrophe bicalyculata (Retz.) Nees leaf extract: Characterization and antibacterial activity," Int. J. Pharm. Sci. Drug Res., vol. 17, no. 4, pp. 354–362, 2025, doi: 10.25004/IJPSDR.2025.170406.
[36] Qamo N. I., Mimouni I., "Preparation and characterization of pure zinc oxide thin films by spray pyrolysis technique," Master's Thesis, Department of Physics, Faculty of Mathematics and Matter Sciences, Kasdi Merbah University of Ouargla, Ouargla, Algeria, 2019–2020, defended on 27 September 2020.
[37] Rahmani S., Wasaa J., "Preparation and study of single and double layers of zinc oxide and nickel oxide by chemical spray pyrolysis technique," Master's Thesis, Department of Physics, Faculty of Mathematics and Matter Sciences, Kasdi Merbah University of Ouargla, Ouargla, Algeria, 2016–2017, defended on 29 May 2017.
[38] Chadala K., "Study of the physical properties of doped zinc oxide (ZnO) thin films prepared by chemical spray pyrolysis technique," Master's Thesis, Department of Physics, Faculty of Mathematics and Matter Sciences, Kasdi Merbah University of Ouargla, Ouargla, Algeria, 2015–2016, defended in May 2016.

تحضير أوكسيد الخارصين باستخدام تقنية الانحلال الحراري بالرش الكيميائي ودراسة خصائصه البصرية

ديانا دريد ابلحد [1] , معتز صالح حسن الجبوري [2]

[1،2] قسم الفيزياء، كلية التربية للعلوم الصرفة، جامعة الموصل، الموصل، العرا ق

المستخلص:

في هذه الورقة البحثية، تمت دراسة الخصائص الهيكلية والبصرية للأغشية الرقيقة من أوكسيد الخارصين التي تم تحضيرها باستخدام تقنية الانحلال الحراري بالرش الكيميائي. وتضمنت عملية الترسيب رش محلول كيميائي شفاف مكون من نترات الخارصين المذابة في ماء مقطر عند درجة حرارة (50°C) على ركائز زجاجية مربعة قياسها (2.5 cm). أجريت عملية الترسيب عند درجة حرارة (350°C) وضغط (2 bar). تمت دراسة الخصائص البصرية لأوكسيد الخارصين باستخدام الأشعة فوق البنفسجية والمرئية عبر نطاق طول موجي من 190 nm إلى 1100 nm. أظهرت النتائج أن قيم الامتصاص أكثر وضوحاً في منطقة الأشعة فوق البنفسجية، بين nm (380-375)، يليها انخفاض حاد في مناطق الضوء المرئي والأشعة تحت الحمراء، حيث أظهرت المادة شفافية عالية. علاوة على ذلك، أظهرت النتائج أن نفس التغير يحدث في معامل الامتصاص والانكسار والخمود والثوابت الضوئية الأخرى كدالة للطول الموجي لأغشية أوكسيد الخارصين. ووجد أن فجوة الطاقة لأغشية أوكسيد الخارصين تبلغ (3.26 eV) عند نفس درجة الحرارة. أظهر قياس حيود الأشعة السينية (XRD) أن بنية مادة أوكسيد الخارصين نقية وسداسية. ساعدنا هذا التحليل في حساب متوسط حجم البلورات، الذي وجد أنه يبلغ تقريباً (44.34nm) وثوابت الشبكة a=b=3.2190 Å و c=5.1490 Å ، وحجم الخلية $46.21 \times 10^6\ pm^3$ ، وكثافة الأشعة السينية لعينة ZnO $5.85\ g/cm^3$ وسماكة الطبقة، وعدد الطبقات $N_L = 6.7658$ ، بينما كانت كثافة الانزياحات $5.086 \times 10^{-4}\ nm^{-2}$، وعدد البلورات $N_\circ = 3.44 \times 10^{11} cm^{-2}$ ، اما فيما يخص المساحة السطحية النوعية $SSA = 24.138\ m^2/g$..